CHAPTER III

RESULTS AND DISCUSSION

In conventional MIP synthesis, MAA and EGDMA were generally used as functional monomer and cross-linker, respectively. However, for each template molecule, optimization of MIP composition is very important in order to obtain highly specific MIP.

In this work, MIP specific to NVP was needed to develop a new assay for NVP determination. The scope of this work was demonstrated in Figure 3.1. Firstly, MIPs were synthesized by varying type and ratio of functional monomers and crosslinkers. The obtained polymers were then screened for NVP binding using UV binding studies. Finally, selected polymers were then used in an assay development.

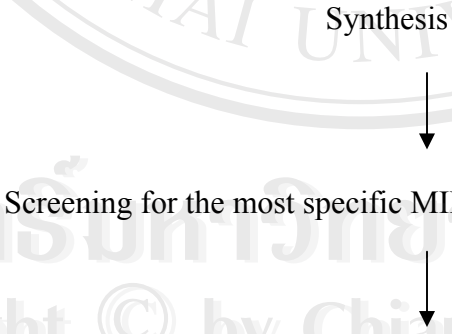

Figure 3.1 Scope of research

3.1 Synthesis of MIPs

Polymers were prepared via self-assembly approach. In the first step, functional monomer and template molecules were mixed together to allow self-assembly between the two molecules. The assembled complex is trapped by polymerizing the monomer together with a cross-linker to form a rigid polymer network. The template removal process was then performed by continuous extraction in a soxhlet extractor.

All polymers prepared in this work were synthesized by free radical polymerization using benzoyl peroxide as an initiator. Structure of templates, function monomers and crosslinkers used for molecular imprinting were shown in Figure 3.2

Various polymers were synthesized by bulk and precipitation polymerization. Polymers synthesized from bulk polymerization have to be crushed into fine powder prior used in the next step. In contrast, polymer obtained from precipitation polymerization can be used without grinding because this method provides microsphere particle.

NIPs were prepared by same procedure without using template molecule.

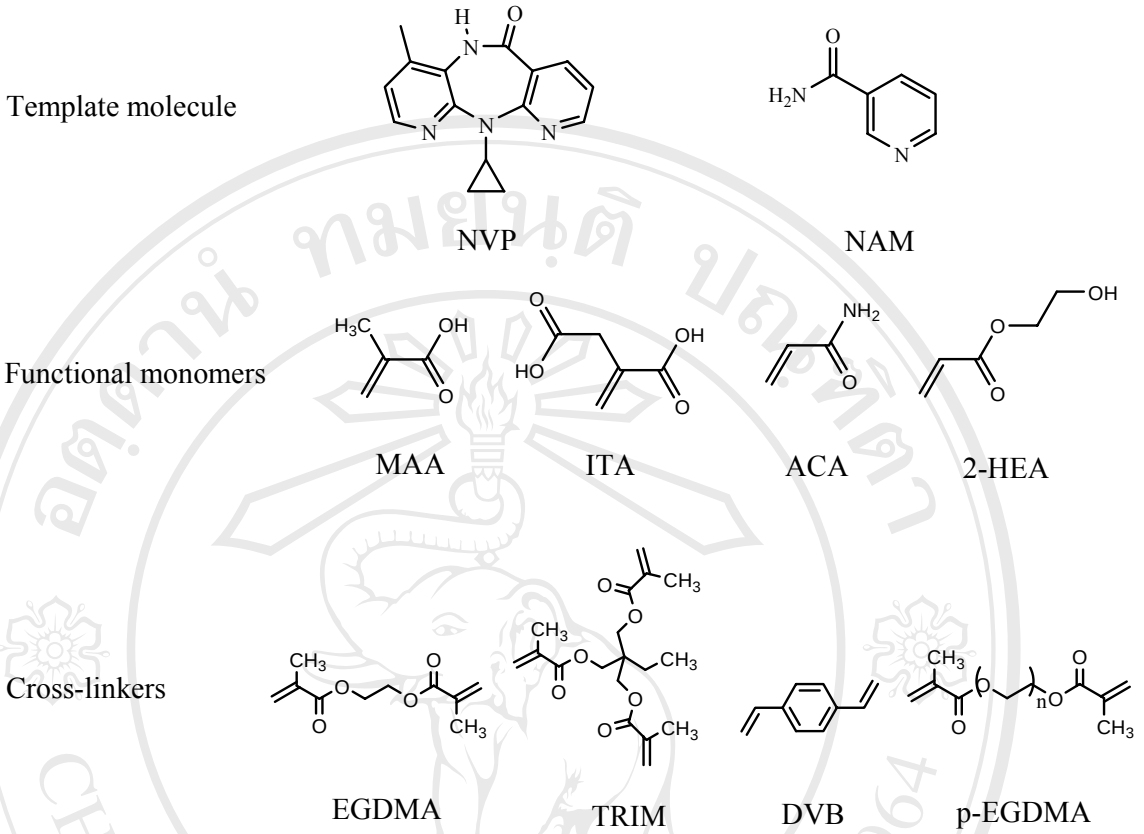

Figure 3.2 Structure of templates, function monomers and crosslinkers used for molecular imprinting.

3.1.1 Synthesis of MIPs using NAM as a template

It has been shown that effective recognition polymer can be prepared by using a compound of similar structure[83]. Due to limited availability of NVP, nicotinamide (NAM) having structure related to NVP was used as a template instead of NVP for the composition optimization. In MIP synthesis, the polymers were prepared by varying parameters including functional monomers (HEA, ACA, ITA, MAA), cross-linkers (EGDMA, TRIM, DVB, p-EGDMA), and porogens (CH_2Cl_2, MeOH:H_2O (4:1, v/v),

THF:MeOH:H_2O (5:4:1, v/v)) (see Figure 3.2). The compositions of these polymers are shown in Table 3.1 and the schematic of NAM-imprinted polymer synthesis is demonstrated in Figure 3.3.

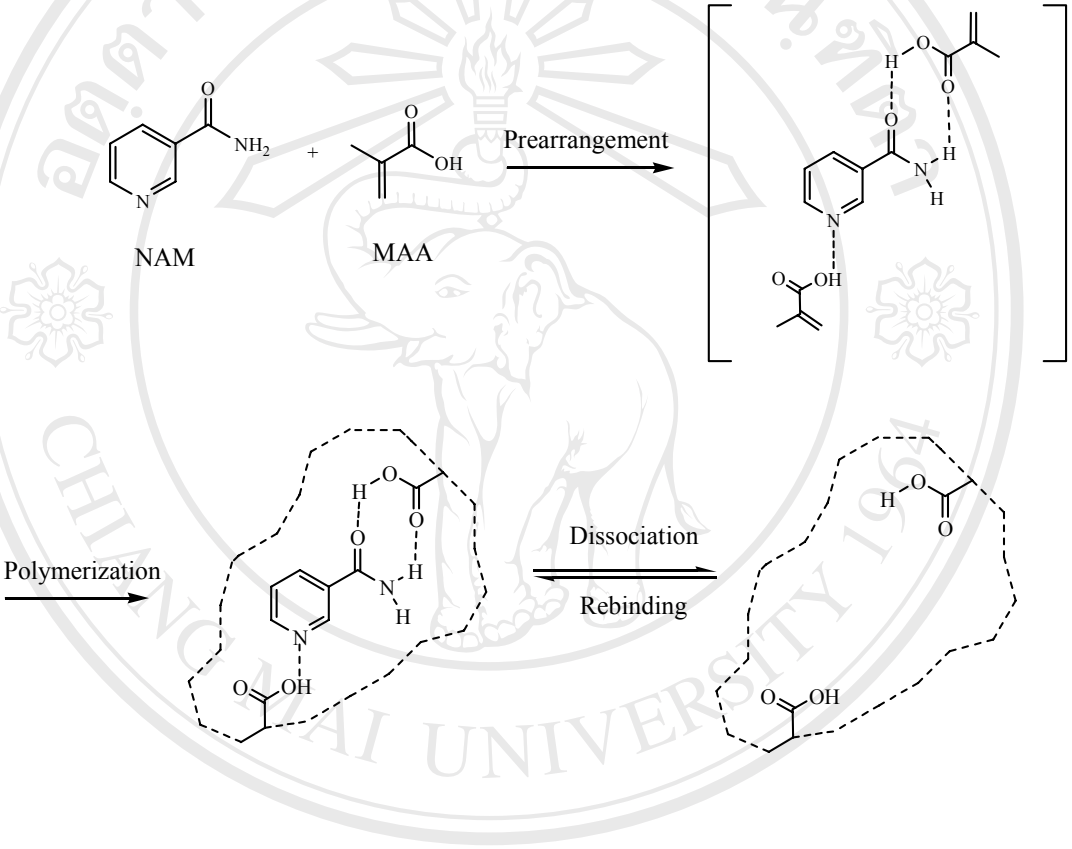

Figure 3.3 Schematic representation of the synthesis of MIPs for NAM

Table 3.1 Composition and percentage yield of MIPs for NAM

Polymer	Template	Function monomers	Cross-linkers	Porogens	Template: monmer: cross-linker	% yield
P1	NAM	ACA	EGDMA	CH_2Cl_2	1:4:20	88
P1'	-	ACA	EGDMA	CH_2Cl_2	1:4:20	92
P2	NAM	HEA	EGDMA	CH_2Cl_2	1:4:20	82
P2'	-	HEA	EGDMA	CH_2Cl_2	1:4:20	89
P3	NAM	ITA	EGDMA	THF	1:4:20	83
P3'	-	ITA	EGDMA	THF	1:4:20	85
P4	NAM	MAA	EGDMA	CH_2Cl_2	1:4:20	83
P4'	-	MAA	EGDMA	CH_2Cl_2	1:4:20	90
P5	NAM	MAA	TRIM	CH_2Cl_2	1:4:20	86
P5'	-	MAA	TRIM	CH_2Cl_2	1:4:20	90
P6	NAM	MAA	DVB	CH_2Cl_2	1:4:20	82
P6'	-	MAA	DVB	CH_2Cl_2	1:4:20	88
P7	NAM	MAA	p-EG	CH_2Cl_2	1:4:4	85
P7'	-	MAA	p-EG	CH_2Cl_2	1:4:4	87
P8	NAM	MAA	TRIM	CH_2Cl_2	1:4:4	82
P8'	-	MAA	TRIM	CH_2Cl_2	1:4:4	90
P9	NAM	MAA	TRIM	CH_2Cl_2	1:4:4	75
P9'	-	MAA	TRIM	CH_2Cl_2	1:4:4	86
P10	NAM	MAA	TRIM	MeOH:H_2O	1:4:4	72
P10'	-	MAA	TRIM	MeOH:H_2O	1:4:4	83
P11	NAM	MAA	TRIM	T:M:H	1:4:4	71
P11'	-	MAA	TRIM	T:M:H	1:4:4	84

Ratio of T:M:H (THF:MeOH:H_2O) = 5:4:1 (v/v)

Ratio of MeOH:H_2O = 4:1 (v/v)

P1-P8 were prepared by bulk polymerization

P9-P11 were prepared by precipitation polymerization

3.1.2 Synthesis of MIP using NVP as a template

After suitable functional monomer, crosslinker and porogen were selected from NAM-imprinted polymers, MIPs using NVP as a template were synthesized accordingly. Compositions and percentage yield of MIPs synthesized are shown in Table 3.2. The representative scheme for the preparation of NVP-imprinted polymers is illustrated in Figure 3.4.

Table 3.2 Compositions and percentage yield of MIPs for NVP

Polymers	Template	Function monomers	Cross linkers	Porogens	Template: monmer: cross-linker	% yield
P12	NVP	MAA	EGDMA	CH_2Cl_2	1:4:20	83
P12'	-	MAA	EGDMA	CH_2Cl_2	1:4:20	87
P13	NVP	MAA	TRIM	CH_2Cl_2	1:4:4	82
P13'	-	MAA	TRIM	CH_2Cl_2	1:4:4	89
P14	NVP	MAA	EGDMA	THF:MeOH:H_2O	1:4:20	79
P14'	-	MAA	EGDMA	THF:MeOH:H_2O	1:4:20	82
P15	NVP	MAA	TRIM	THF:MeOH:H_2O	1:4:4	80
P15'	-	MAA	TRIM	THF:MeOH:H_2O	1:4:4	84
P16	NVP	ITA	TRIM	THF:MeOH:H_2O	1:4:4	78
P16'	-	ITA	TRIM	THF:MeOH:H_2O	1:4:4	86

Ratio of THF:MeOH:H_2O = 5:4:1 (v/v)

P12-P13 were prepared by bulk polymerization

P14-P16 were prepared by precipitation polymerization

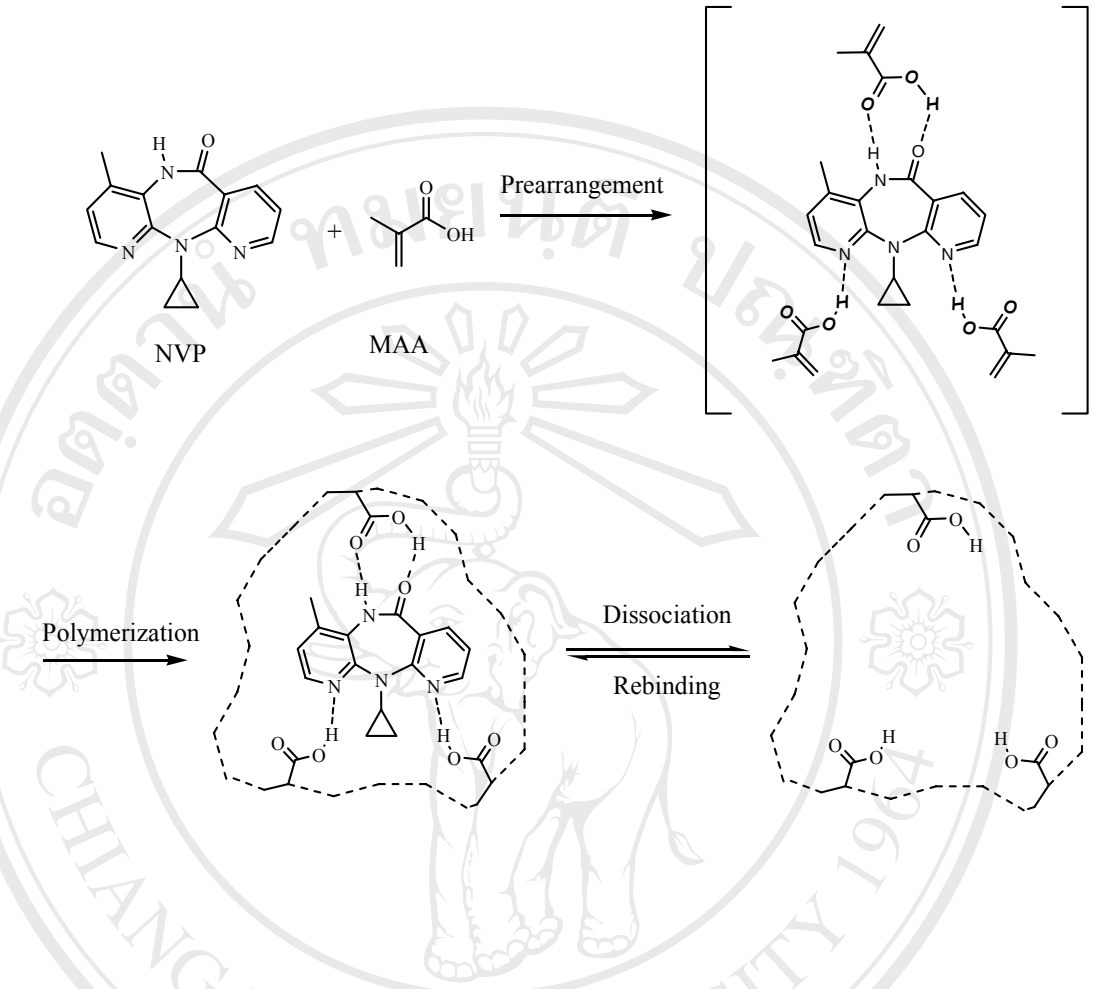

Figure 3.4 Schematic representation of the synthesis of MIPs for NVP

3.2 UV binding studies

The recognition ability of the imprinted polymer was investigated by equilibrium binding experiments. The rebinding of template molecule was performed in both organic and aqueous solvents. In brief, the powder polymer was added into a solution of template. The resulting suspension was incubated for 24 h. and the quantity of the analyte in solution was determined by UV spectroscopy (λ_{max} = 262 and 281 nm for NAM and NVP, respectively). The amount of analytes bound to the polymer, Q, was calculated by

subtracting the concentration of free analytes from the initial loading. Percent bound of analyte was calculated according to the equation, % Bound = $(Q/Q_{initial})$ x 100. Imprinting factor (α) was defind as the ratio of the adsorbed amounts of analyte by the MIPs to the one by the NIPs.

3.2.1 UV binding with nicotinamide (NAM)

The obtained polymers (P1-P11) were used for UV binding study in organic and aqueous medium in order to select suitable polymer composition to be used in the synthesis of NVP-imprinted polymers. The binding of MIPs to NAM was evaluated in comparison with NIPs. Percent bound of NAM by the polymers were shown in Figure 3.5 and the imprinting factors of MIPs were shown in Table 3.3.

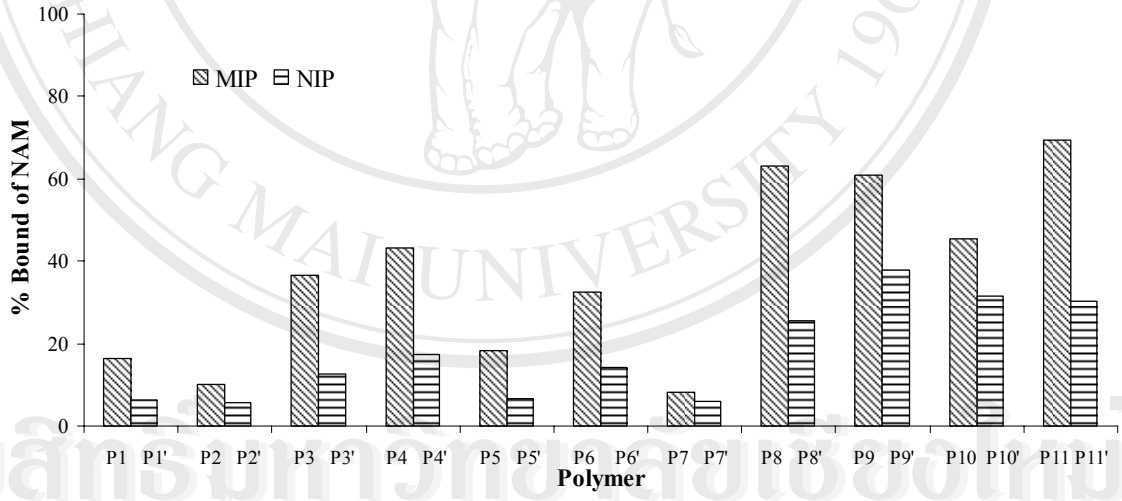

(a) ACN

Figure 3.5 Comparison of % bound of polymers P1-P11 to NAM (0.5 mM) in (a) ACN with 40.0 mg/ml polymer (b) buffer pH 7 with 40.0 mg/ml polymer (c) buffer pH 7 with 20.0 mg/ml polymer

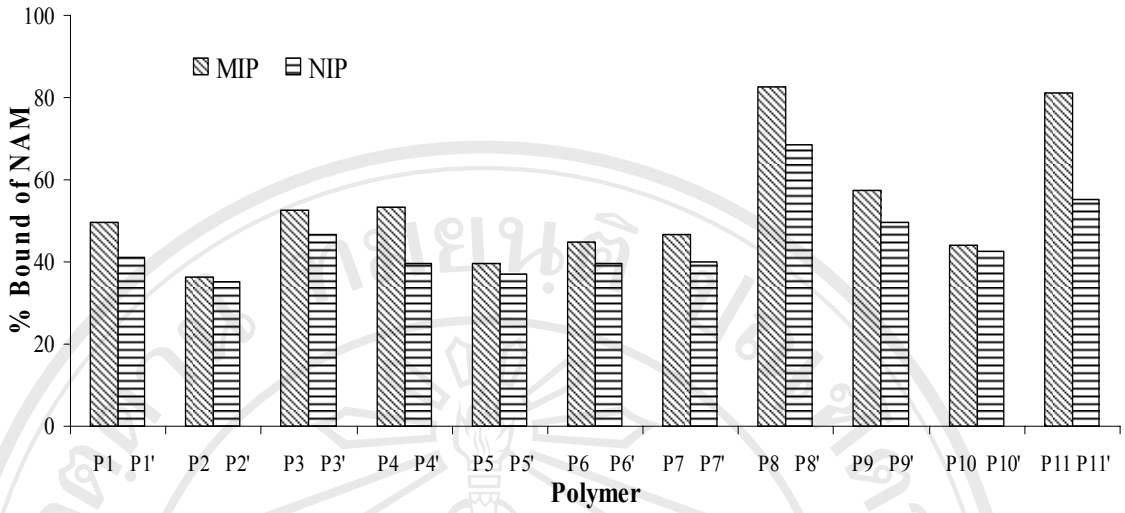

(b) Buffer pH 7

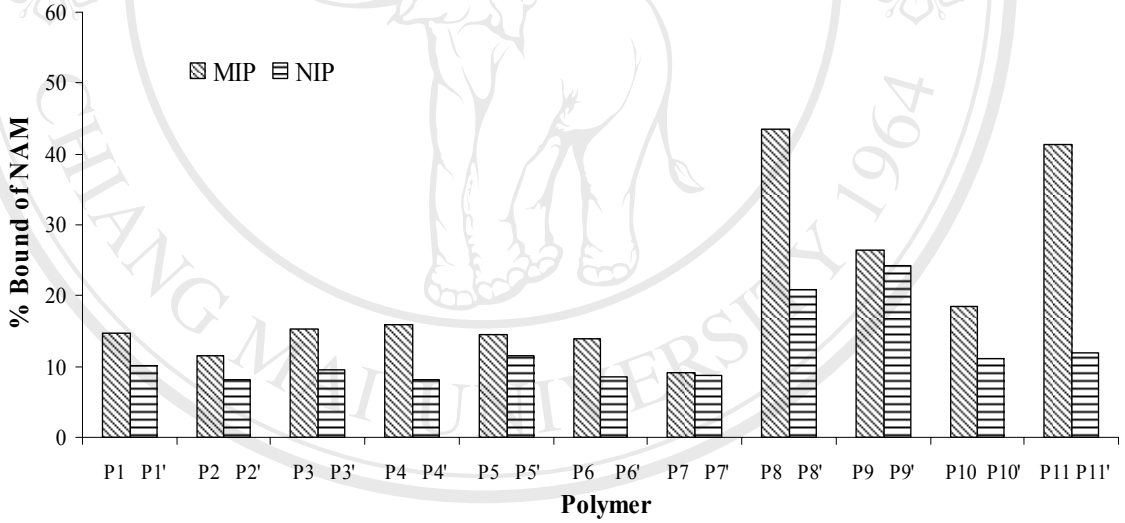

(c) Buffer pH 7

Figure 3.5 (continued)

Table 3.3 Imprinting factor of P1-P11

Polymer	Imprinting factor (α)		
	ACN (40.0 mg polymer)	**Buffer pH 7 (40.0 mg polymer)**	**Buffer pH 7 (20.0 mg polymer)**
P1	2.66	1.20	1.44
P2	1.82	1.03	1.40
P3	2.93	1.12	1.59
P4	2.23	1.34	1.94
P5	2.79	1.07	1.25
P6	2.31	1.13	1.62
P7	1.33	1.16	1.04
P8	2.57	1.20	2.52
P9	1.61	1.16	1.09
P10	1.44	1.04	1.65
P11	1.97	1.46	3.27

Figure 3.5 (a) showed NAM binding of the polymers in ACN. Among the P1-P4 synthesized under bulk polymerization with different functional monomers, P4 exhibited highest binding to NAM while P3 showed the highest imprinting factor.

Effect of cross-linkers can be seen in the binding ability of P4-P9 synthesized by bulk polymerization with various types of crosslinkers. Polymer P8 using TRIM as the cross-linker (1:1 ratio with monomer) was the most effective polymer in binding to NAM and showed high imprinting factor. P5 although showed the highest imprinting factor, this polymer exhibited low binding ability to NAM. This result suggests that P5 contains

a higher number of specific binding sites in comparison with its corresponding NIP (P5') but lower number of binding sites when comparing with the other polymers.

Comparing percent bound of NAM by polymers P9-P11 synthesized by precipitation method in various porogens, it was found that P11 synthesized by mixing solvent of THF:MeOH:H_2O (5:4:1, v/v) showed maximum percentage bound to NAM and also has maximum imprinting factor. Addition of less polar solvent such as THF seems to give better non-covalent complexation between monomer and template resulting to a more effective imprinting.

Effect of polymerization methods can be seen when comparing polymer P8 and P9 synthesized by bulk and precipitation method, respectively. It was found that P8 showed maximum percentage bound to NAM and also has maximum imprinting factor. This implies that P8 has more number of specific binding sites to NAM than P9 under this condition.

The binding abilities of polymers P1-P11 and their NIPs in phosphate buffer pH 7 were shown in Figure 3.5 (b). The results showed that there was no difference in percent bound of MIPs when compared with the data from NIPs. It is noted that all polymers exhibited high binding ability to NAM, especially polymers P8 and P11 which bound nearly 100 percent of NAM. However, imprinting factors of all MIPs were lower in this solvent system in comparison with ACN. This result implies that in an aqueous media, hydrophobic interaction seems to enhance nonspecific binding of these polymers. As a result, binding of MIP and NIP cannot be differentiated under this condition.

When the amount of polymers is decreased to 20 mg/ml (Figure 3.5 (c)), the difference between the binding ability of MIP and NIP can be observed. The results

showed that P8 and P11 exhibited high binding ability to NAM and P11 also exhibited the highest imprinting factor.

It can be concluded that polymers P3, P4, P8 and P11 exhibit high binding abilities and imprinting factors both in organic and aqueous solvents. The experimental conditions used in preparing these polymers where therefore used to synthesize nevirapine-imprinting polymers in which their binding ability were evaluated in the following section.

3.2.2 UV binding with nevirapine (NVP)

Polymers P12-P16 using NVP as a template were used to evaluate NVP binding efficiency in organic and aqueous solvents. Percent bound of NVP by the polymers are shown in Figure 3.6 and the imprinting factors of MIPs are listed in Table 3.4.

Figure 3.6 (a) showed binding abilities of P12-P16 in ACN. It was found that P15 showed maximum percentage bound when compared with other polymers. Although P12 gave highest imprinting factor, it exhibited low binding to NVP.

The binding abilities of all polymers in phosphate buffer pH 7 are shown in Figure 3.6 (b). All polymers showed very high binding to NVP and have low imprinting factors probably due to hydrophobic effect. Nevertheless, when the amount of polymer was decreased to 5.0 mg/ml (Figure 3.6 (c)), the difference of percent bound among MIPs and NIPs can obviously be distinguish. It was found that P15 gave highest percent bound to NVP and imprinting factor.

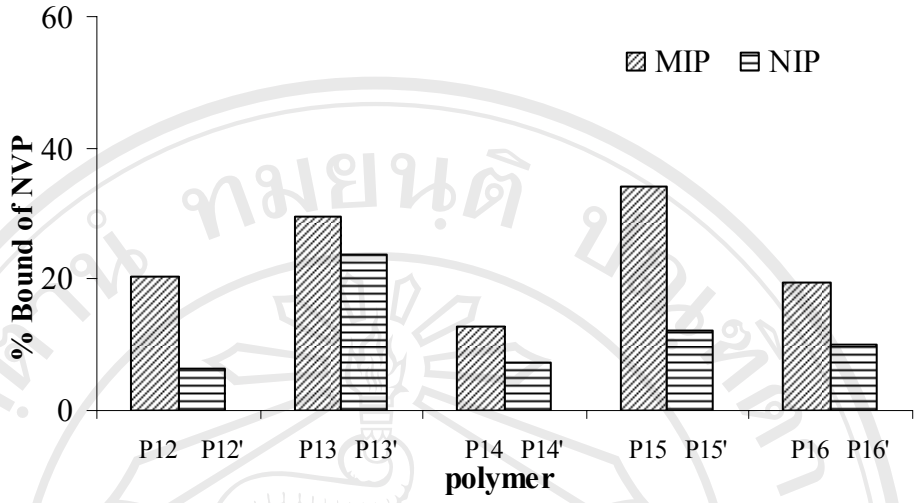

(a) ACN

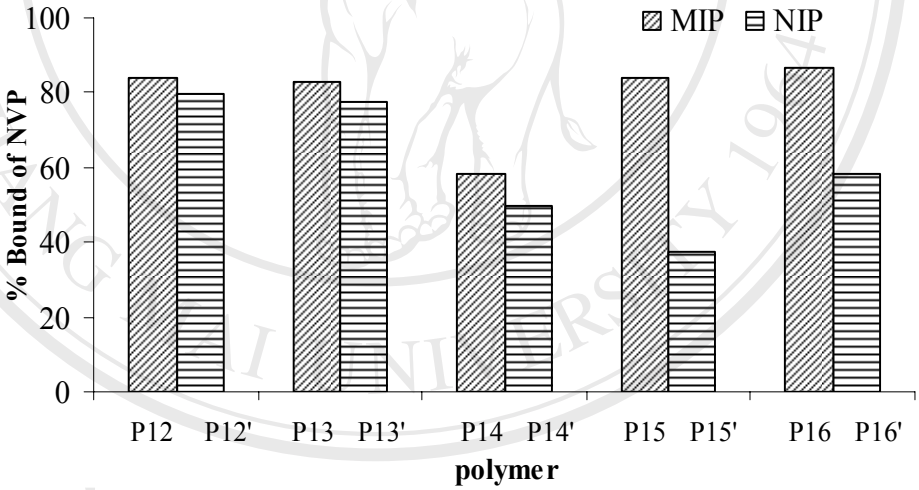

(b) Buffer pH 7

Figure 3.6 Comparison of % bound of polymers P12-P16 to NVP (0.2 mM) in (a) ACN with 20.0 mg/ml polymer (b) buffer pH 7 with 20.0 mg/ml polymer (c) buffer pH 7 with 5.0 mg/ml polymer

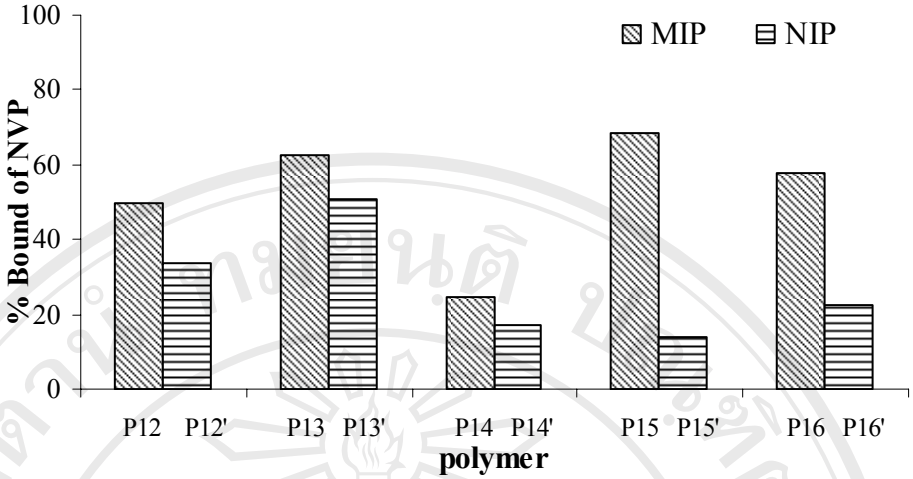

(c) Buffer pH 7

Figure 3.6 (continued)

Table 3.4 Imprinting factor of P12-P16

Polymer	Imprinting factor (α)		
	ACN 20.0 mg polymer	Buffer pH 7 20.0 mg polymer	Buffer pH 7 5.0 mg polymer
P12	3.16	1.05	1.16
P13	1.25	1.16	1.23
P14	1.73	1.06	1.43
P15	2.75	2.25	4.85
P16	1.80	1.49	2.57

3.3 Characterization of NVP-imprinted polymers

Selected polymers synthesized in section 3.1 were characterized by scanning electron microscope (SEM) and FT-IR techniques.

3.3.1 Scanning electron microscopy (SEM)

Methods of polymerization are main factor that govern morphology of polymers synthesized. In this study two methods of polymerization were used to prepare MIPs. These methods are bulk polymerization and precipitation polymerization. Size and shape of NVP imprinted polymers prepare by these methods were compared using SEM technique. Representative SEM images of P13 and P15 are shown in Figure 3.7. Bulk polymerization (P13), grinding the polymer monolith showed agglomerated polymeric material in irregular shapes with rough surface in the size range of 5–15 μm (Figure 3.7 (a and b)). In the case of precipitation method (P15), the polymeric material produces colloidal particle with a regular spherical shape and a size range of 100-200 nm (Figure 3.7 (c)).

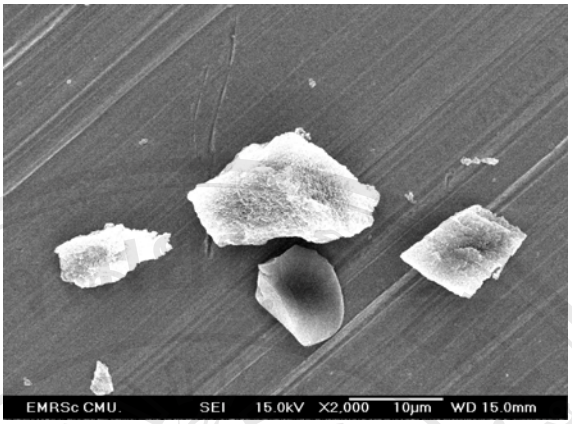

(a)

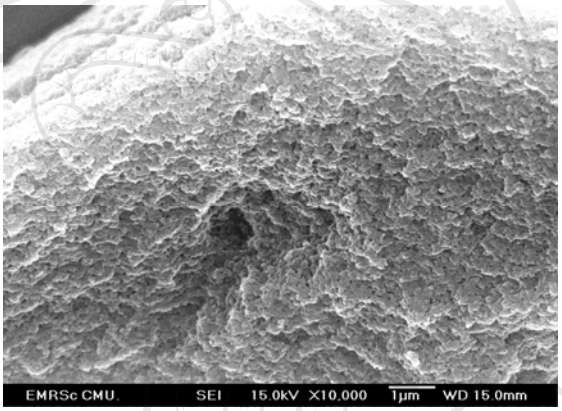

(b)

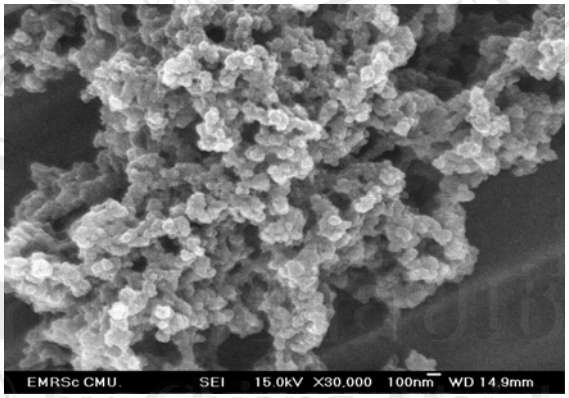

(c)

Figure 3.7 SEM image of (a) irregularly shaped P13 with 2000x magnification, (b) P13 with 10000x, and (c) P15 with 30000x magnification.

3.3.2 Fourier transform infrared (FT-IR)

In this study, FT-IR was used for characterization of MIP and NIP polymers. The samples for FT-IR analysis were prepared in form of KBr discs. As can be seen in Figure 3.8 and Table 3.5 the representative FT-IR spectra of P15 and P15' are very similar. This confirmed that the P15 has the same chemical component as P15' and the template molecule can be removed from the polymer matrix.

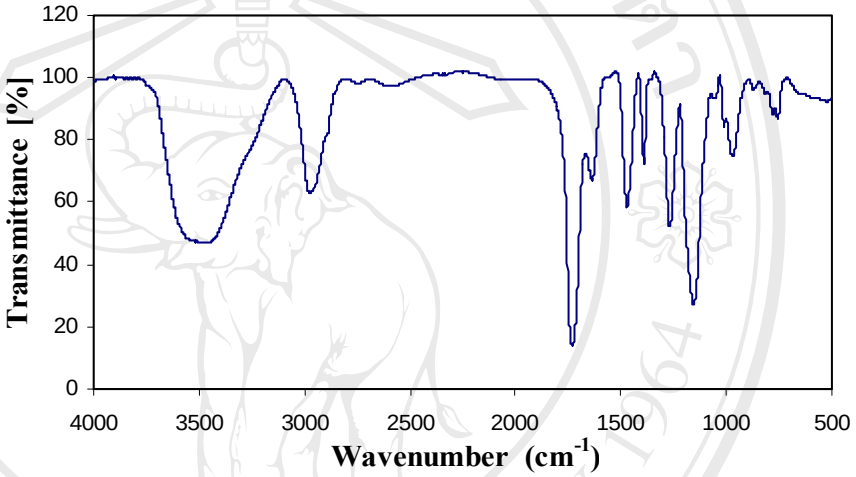

(a)

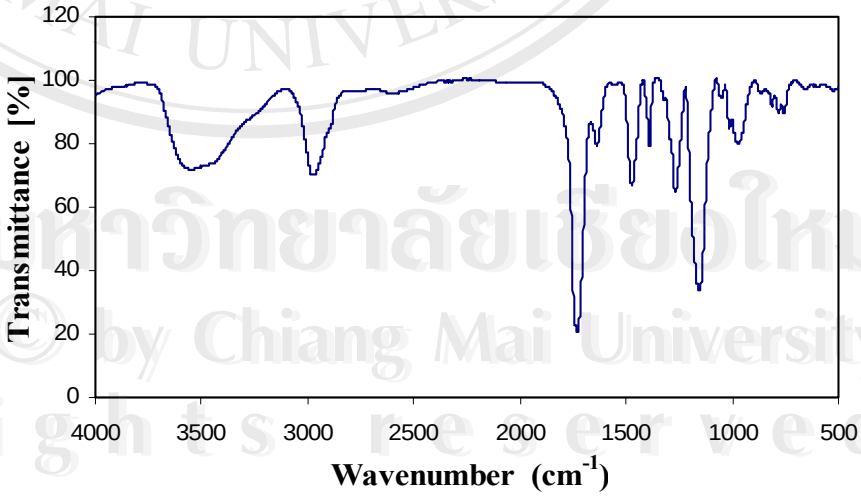

(b)

Figure 3.8 FT-IR spectrum of (a) P15 and (b) P15'

Table 3.5 Vibrational assignment and wavenumber in the infrared spectrum of P15 and P15'

Vibrational assignment	Wavenumber (cm^{-1})	
	MIP (P15)	NIP (P15')
O-H stretching	3472	3485
C-H stretching	2954	2947
C=O stretching	1724	1722
C-H bending	1463, 1386	1465, 1386
C-O stretching	1150	1147

3.4 Selectivity of P11 and P15

The polymer P11 and P15 were used for the selectivity test that were carried out using a series of structurally related compounds of NVP including NAM, BAM, 2-Apy, 3-Apy, 4-Apy, pyridine, aniline and OPD (see Figure 3.9). The amounts bound to MIPs (P11 and P15) and their corresponding NIPs were determined by the rebinding of 0.2 mM of each compound in 0.01 M phosphate buffer, pH 7 containing 0.05% tween 20. The distribution coefficients of the selected analytes between solution and polymer were calculated and list in Table 3.6. The distribution coefficient Kd is defined as:

$$Kd = Cp/Cs$$

Where Cp = concentration of analyte on the polymer (in μmol g^{-1}) and Cs = concentration of analyte in the solution (in μmol ml^{-1}).

The results of these studies are shown in Figure 3.10 and Table 3.6. P11 exhibited higher percent bound to NVP than its template and other substrates. The highest Kd value for NVP of this polymer suggested that P11 exhibited high binding specificity toward NVP. This could be explained by the fact that NVP contains pyridine ring and amide group as in NAM. Both of these groups seem to cooperatively interact with the carboxyl groups in binding sites of the polymer in forming two strong hydrogen bonds. Another reason that could enhance binding ability of P11 to NVP is probably due to hydrophobic driving force of the less polar NVP in comparison with NAM.

For P15, among all substrates, the polymer exhibited the highest Kd value for NVP. Nevertheless, it can be seen that polymer not only showed high percent bound to its template NVP but also bound to NAM with high affinity. This finding is as expected since NAM structure represents half of the NVP structure.

The obvious difference of binding specific between MIPs (P11, P15) and NIPs for NVP mainly results from the carboxyl functional groups within the microcavities created in the MIPs matrix by imprinting which are complementary both in shape and the functional group arrangement to the template molecule (NVP). Although, NIPs has the same chemical composition as MIPs, it does not have the recognition sites complementary in both shape and functional groups to those of NVP and the arrangement of carboxyl groups in NIPs are random.

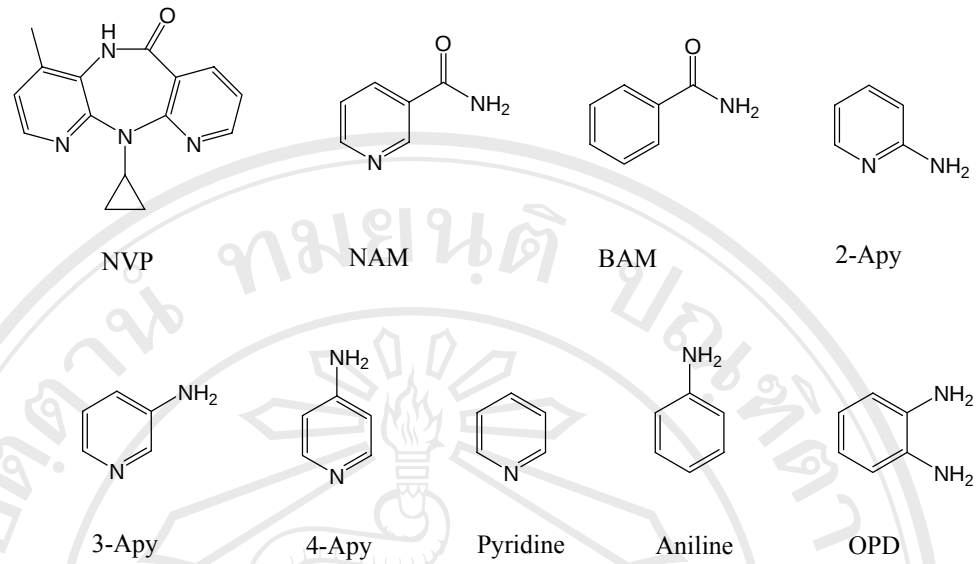

Figure 3.9 Structure of compounds used in selectivity studies.

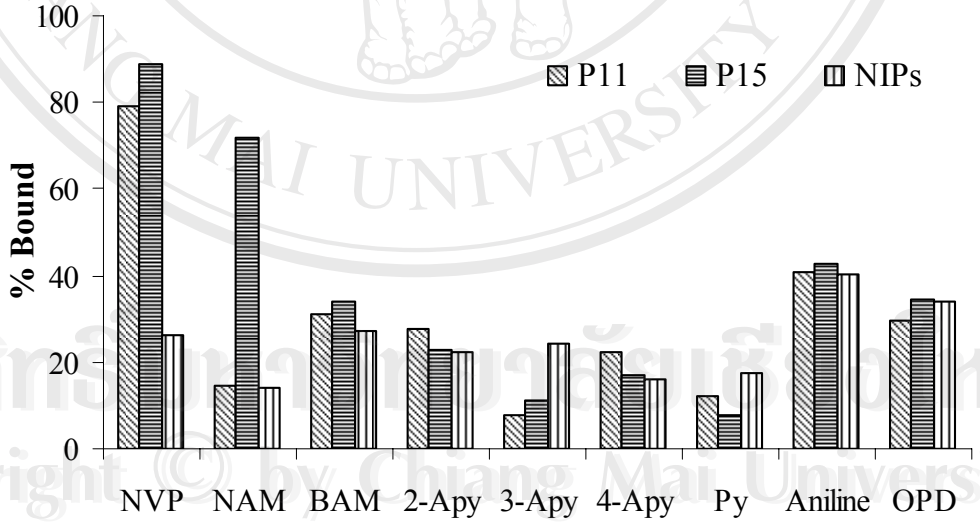

Figure 3.10 Percent bound of NVP and its structurally related compounds to P11, P15 and NIPs; polymers: 5.0 mg; V = 1.0 ml; Adsorption time: 1.0 h.

Table 3.6 The distribution coefficient (K_d) of P11, P15 and NIP

Substrates	K_d		
	P11	**P15**	**NIP**
NVP	756.09	1611.34	71.04
NAM	34.54	508.42	32.87
BAM	90.56	102.22	74.26
2-Apy	75.70	58.52	57.51
3-Apy	17.19	24.94	63.74
4-Apy	56.80	40.75	37.90
Pyridine	27.67	16.53	41.89
Aniline	137.62	148.82	135.90
OPD	83.94	106.21	103.02

Unit: ml g^{-1}; polymer 5.0 mg/ml. [initial substrate] = 0.2 mmol/L; V = 1.0 ml; adsorbtion time 1.0 h.

3.5 Assay development by competitive ELISA

Assays using MIPs in place of bio-antibodies are called molecular imprinted sorbent assays (MIAs). Most MIAs developed so far have employed radiolabelled probes[57-61]. However, this involves the handling of radioactive materials and produce radioactive waste, which is highly undesirable. On the other hand, enzyme probes although are the most common probes used in ELISA, only limited works have been investigated the application of this type of probe in MIAs. Since enzyme has been proven to be very effective in the typical immunoassays, in this study, enzyme labelled probe was selected to be used in an assay development for NVP detection.

Methods in the development of enzyme-linked binding assays (ELISA) for NVP detection are as followed. Firstly, suitable polymers were selected from the UV binding studies. Enzyme-linked nevirapine was then synthesized and characterized by competitive ELISA. Finally, an ELISA assay using the selected polymer and the synthesized enzyme conjugate was then developed and evaluated.

3.5.1 Synthesis of NVP-HRP conjugate

NVP-HRP conjugate was synthesized according to Scheme 1. The amide of NVP was reacted with methyl-5-bromovalerate to form NVP-linked ester compound **1**. After base hydrolysis of the esters, NVP-linked carboxylic acid, compound **2,** was obtained. The corresponding NHS activated ester generated *in situ* was then reacted with HRP to generate the NVP-HRP conjugate**.**

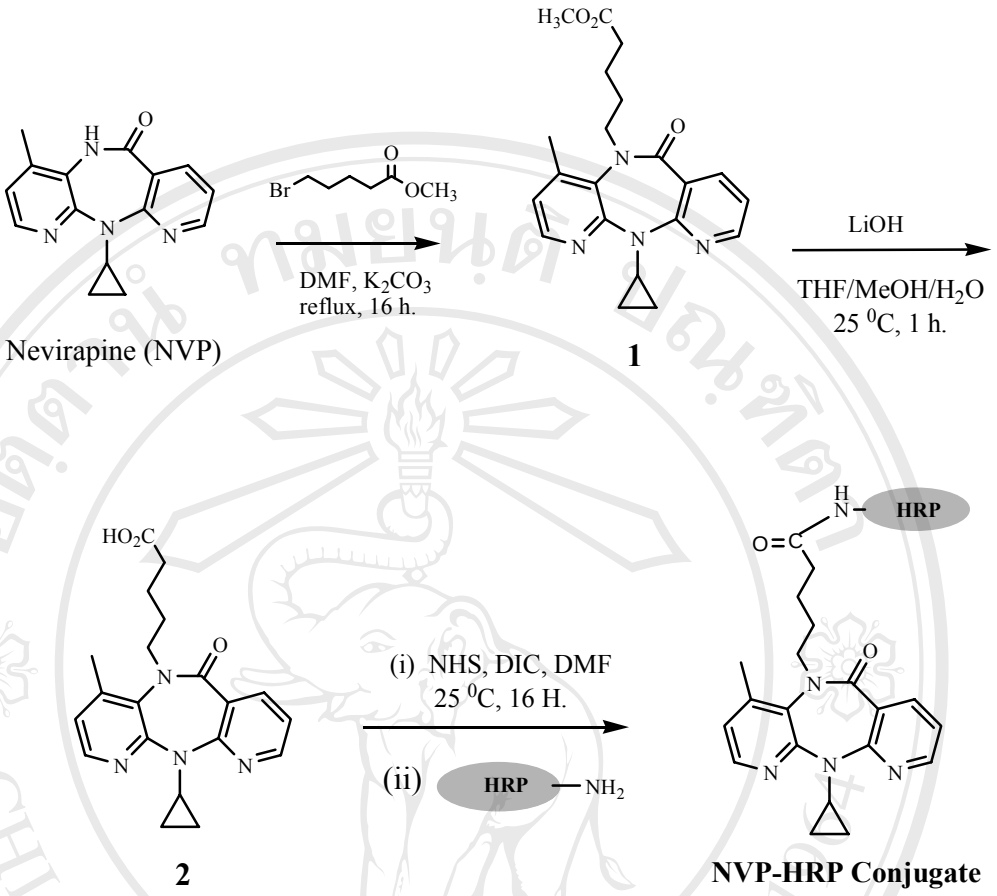

Scheme 3.1 Synthesis of NVP-HRP conjugate

3.5.2 Characterization of NVP-HRP conjugate by competitive ELISA

To confirm the presence of NVP in the enzyme conjugate, the synthesized NVP-HRP conjugate was characterized by competitive ELISA using rabbit anti-NVP antibodies prepared from separated work[75].

The competition of NVP-HRP conjugate and NVP (10, 1.0, 0.1, 0.01 μg/ml and non-inhibition) is shown in Figure 3.11. From the calibration curve, it was found that NVP can compete with NVP-HRP conjugate (1: 4000 dilution) in a range of 0.01-1.0

μg/ml. This data suggests that NVP-HRP conjugate was successfully produced and should be suitable for establishment of an MIA in the next experimental step.

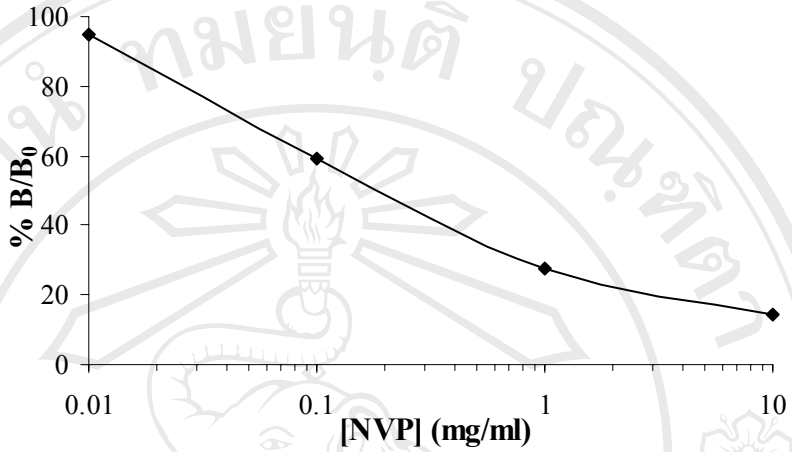

Figure 3.11 Calibration curve for NVP detection using rabbit anti-NVP antibodies

3.5.3 Development of enzyme linked sorbent assay using P11 and P15

3.5.3.1 Effect of additive surfactant

In the preliminary experiments, it was found that NVP-HRP conjugate bound to the polymer if no surfactant was added. Effect of additive surfactant was therefore studied to minimize non-specific binding due to hydrophobic interactions of protein with the polymer.

Figure 3.12 showed percent bound of enzyme conjugate to MIP (P11 and P15) and NIP with and without addition of tween 20. It was found that without tween 20, enzyme conjugate bound non-specifically to both MIP as well as NIP. When using 0.05% tween 20, binding of the conjugate to the NIP was much lower than that to the

imprinted polymer. This data suggested that hydrophobic interaction between MIP and the enzyme conjugate was reduced when adding tween 20.

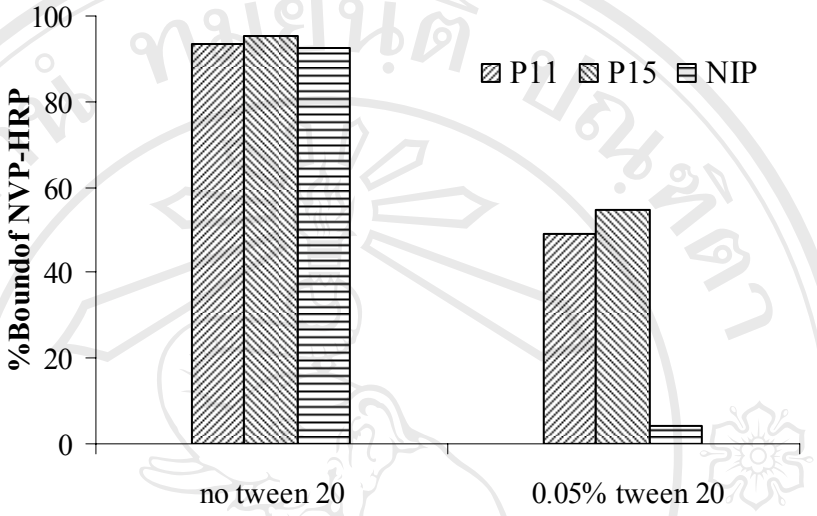

Figure 3.12 Percent bound of enzyme conjugate to P11, P15 and NIPs with and without tween 20

3.5.3.2 Determination of an IC_{50}

The suitable amount of polymers that can bind 50% of enzyme labelled (IC_{50}) was determined by titration experiments. In these studies, various amount of polymers was incubated with an appropriate concentration of NVP-HRP (1:500,000 dilution) in 0.01 M phosphate buffer at pH 6, 7 and 8. The amounts of unbound NVP-HRP in supernatant were then determined by colorimetric detection (λ_{max} = 450 nm) using TMB as substrate. The results are shown in Figure 3.15.

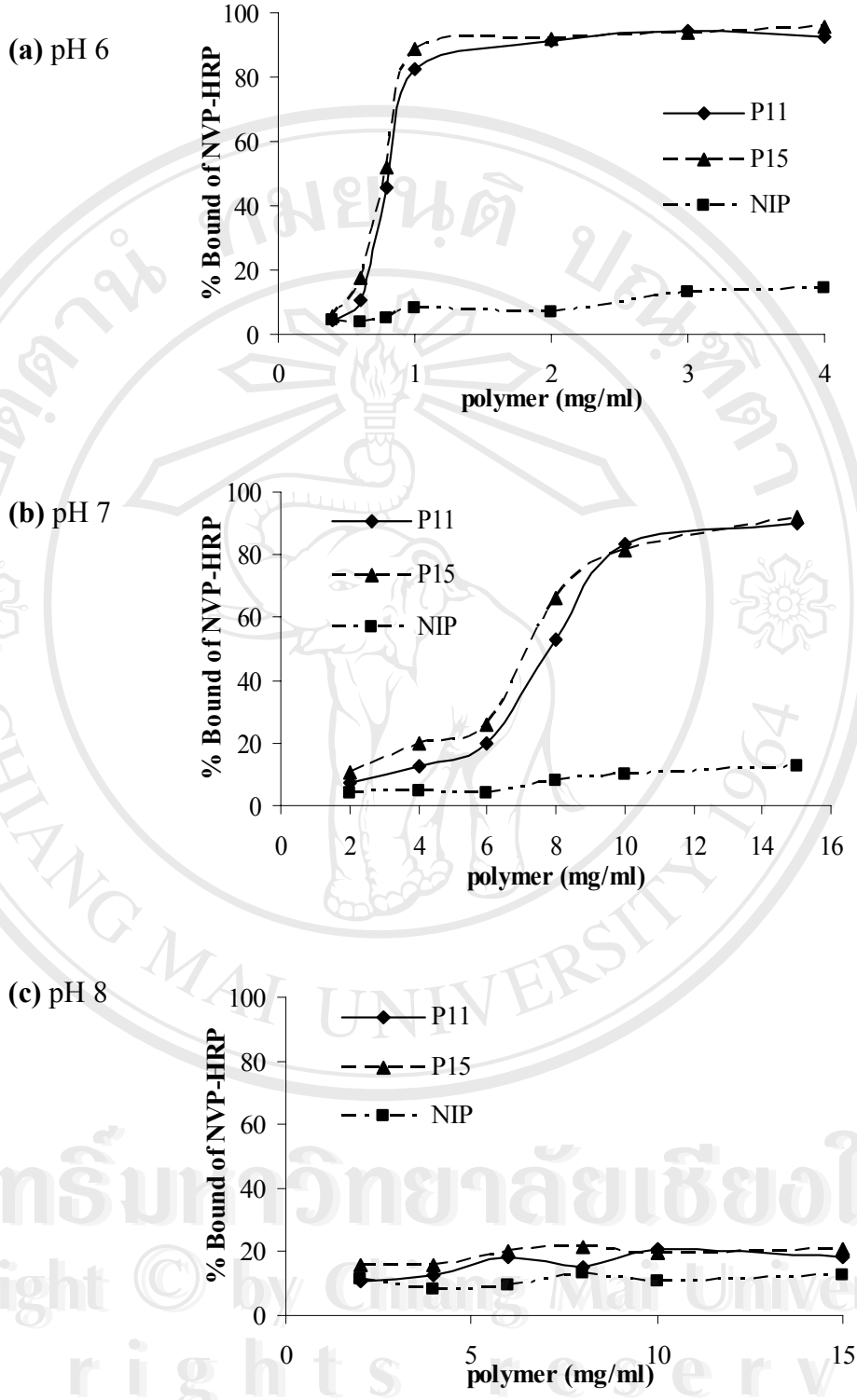

Figure 3.13 Binding of NVP–HRP relative to polymer concentration for P11, P15, and NIP; (a) pH 6, (b) pH 7 and (c) pH 8

It was found that at pH 6, IC_{50} of P11 and P15 were 0.8 mg/ml (Figure 3.13 (a). At pH 7, IC_{50} of P11 and P15 were 8.0 mg/ml and 7.0 mg/ml, respectively (Figure 3.13 (b). In case of pH 8 (Figure 3.13 (c)), no significant binding of NVP-HRP was observed for all polymers.

Since binding condition at pH 6 requires the least amount of polymer, this parameter was adopted in the following step.

3.5.3.3 Binding characteristics and Scatchard analysis of P11 and P15 with NVP in 0.01 M phosphate buffer pH 6

To ensure that NVP can bind to the polymer under the same condition used in the binding of the enzyme conjugate, binding isotherms of polymers P11 and P15 were determined in NVP concentration range of 25-500 μg/ml. Figure 3.14 (a) showed the binding of NVP at various concentrations. The data showed that the amount of NVP bound to polymer was directly dependent on the concentration of NVP. Linearity range was observed for NVP concentration up to 200 μg/ml for both polymers. In this range, the obtained binding data were plotted according to the Scatchard equation[84,85] to estimate the binding parameters of P11 and P15.

$$Q/[NVP] = (Q_{max} - Q/K_d) \qquad (1)$$

where K_d is dissociation constant and Q_{max} an apparent maximum number of binding sites. The results indicate that the Scatchard plot is a line (Figure 3.14 (b)), the slope and intercept of which are equal to $-1/K_d$ and Q_{max}, respectively, and that the binding sites in P11 and P15 are homogeneous with respect to the affinity for NVP,

which were formed due to template effect in the imprinting process and that the non-specific adsorption to both polymers could be assumed to be small enough to ignore in this concentration range. The Q_{max} and K_d values can be calculated to be 57.92 μg/mg and 134.27 mg/ml for P11 and 95.62 μg/mg and 166.72 mg/ml for P15. These data show that P15 exhibited higher binding capacities and strong binding to NVP than P11.

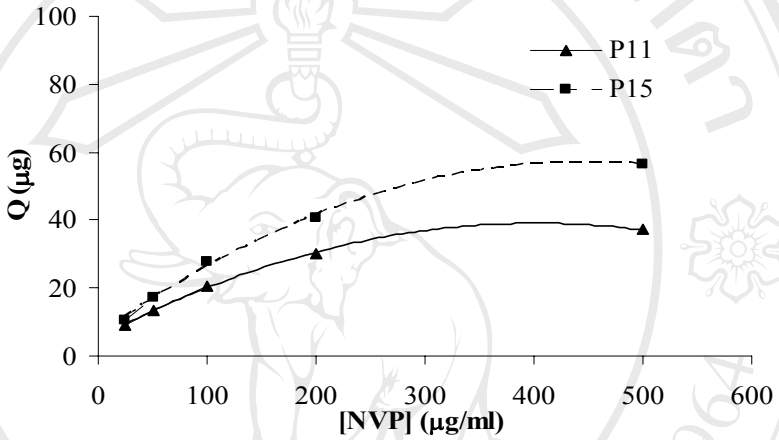

(a)

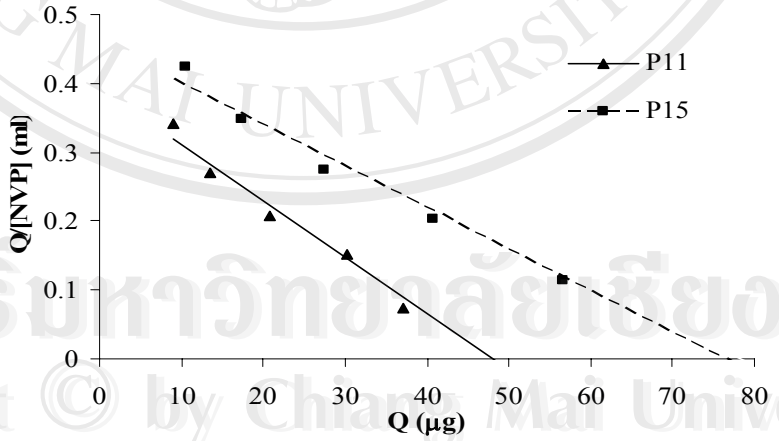

(b)

Figure 3.14 Binding isotherm (a), Scatchard plots (b) of P11 and P15; Q: amount of NVP bound to 0.8 mg of polymers; *V* = 1.0 ml; Adsorption time: 1.0 h.

3.5.3.4 The competitive ELISA

After obtained the suitable assay conditions, the competitive ELISA was performed using P11 and P15 by varying amount of free NVP (0.1-500 μg/ml) with an appropriate amount of NVP-HRP conjugate.

When using high dilution of enzyme labeled analyte (1:500,000), the absorbance activity of the initial NVP-HRP conjugate in supernatant can be measured. By substracting the concentration of the unbound NVP-HRP from the initial NVP-HRP concentration, the amount of NVP-HRP conjugate bound to the polymer can be obtained. Figure 3.15 shows the calibration curve that is plotted in terms of % B/B_0 and [NVP] (logarithmic scale); B and B_0 represent the bound enzymatic activity in the presence and absence of competitor, respectively. It was shown that NVP can compete with NVP-HRP conjugate only slightly at high concentration. Thus, under this condition the calibration curve for detection of NVP cannot be obtained. The reason for this is because the enzymatic activity signal in the presence and absence of NVP has a very slight difference.

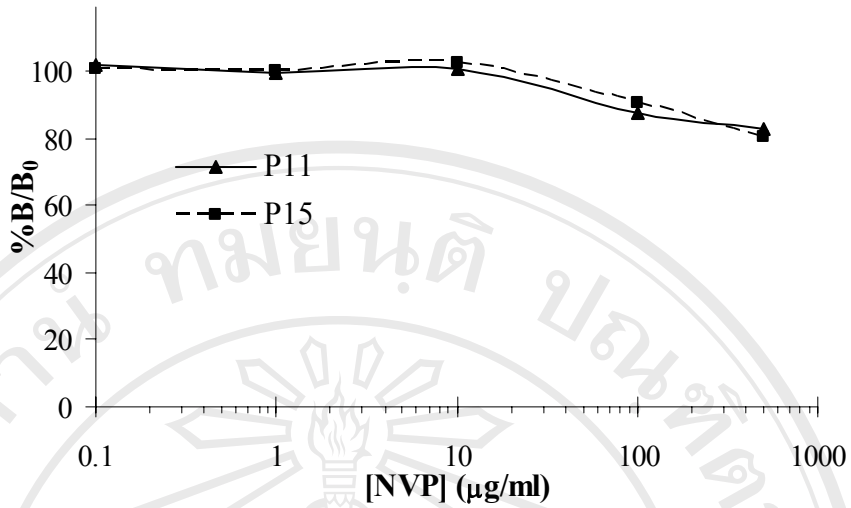

Figure 3.15 Displacement curve with unblabelled NVP as competitor using 1:500,000 dilution of NVP-HRP conjugate

When the concentration of NVP-HRP conjugate was increased to 1:20,000 dilutions, the initial enzyme concentration could not be measured. Therefore, the calibration curve from this experiment was plotted between ΔAbs. and NVP concentration, where ΔAbs. is the difference of absorbance of the enzymatic activity in the presence and absence of NVP in supernatant.

Figure 3.16 shows the calibration curve for NVP in a competitive assay format. Free NVP effectively competed with NVP-HRP conjugate in the binding site of imprinted polymer. The linearity range for NVP detection is 10-300 μg/ml and 100-400 μg/ml using P11 and P15, respectively. Interestingly, under this condition polymer P11 gave lower limit of detection than P15. It may be due to P15 has higher NVP loading than P11, therefore higher concentration of NVP is needed in competition with enzyme labeled NVP.

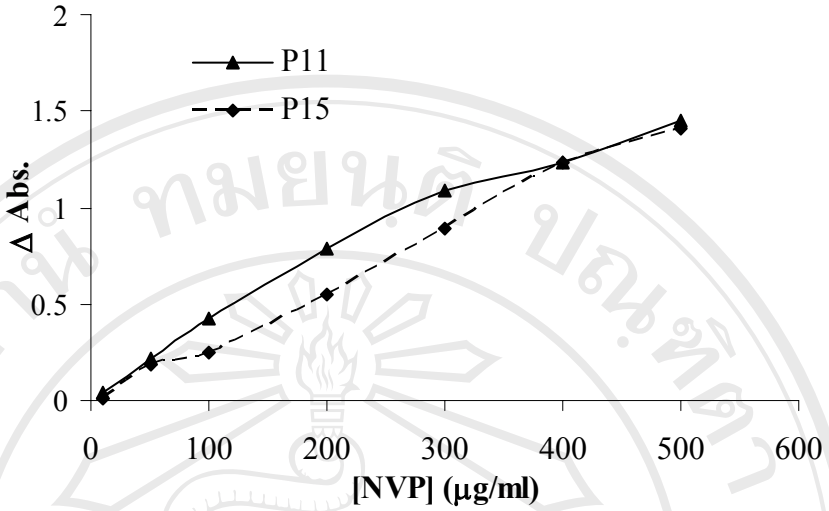

Figure 3.16 Displacement curve with unblabelled NVP as competitor using 1:20,000 dilution of NVP-HRP conjugate